Time delay compensation in bilateral teleoperations using IMPACT

Time Delay Compensation in Bilateral Teleoperations Using IMPACT

Alper Denasi, Dragan Kostić, *Member, IEEE* and Henk Nijmeijer *Fellow, IEEE*

***Abstract*—Teleoperated systems may be subject to destabilizing and performance degrading effects due to time-delays. An appealing remedy is an application of the Internal Model Principle And Control Together (IMPACT) structure as it is done in this paper in the problem of position error based bilateral teleoperation. The IMPACT algorithm proposed in this paper allows time-delay compensation and rejection of disturbances from a known class that act at the output of the slave manipulator. Simulation and experimental results illustrate the effectiveness of the algorithm.**

***Index Terms*—IMPACT structure, position error based bilateral teleoperation, disturbance rejection, time delay compensation, robust stability, Smith predictor.**

I. INTRODUCTION

TELEOPERATED systems are a popular research subject in the robotics community for several decades. They are utilized in applications that take place in hazardous environments such as nuclear power plants for nuclear waste disposal, in hospitals to perform minimally invasive surgery, in space to perform repair of orbital modules, etc [1]. For a more extensive survey about the developments in this field the interested reader is refered to the references [1], [2]. The teleoperated tasks are carried out by a slave manipulator located at a remote environment. The slave receives commands sent by a human operator through a communication channel. As the name suggests, when bilateral teleoperations are considered, the sensor data from the slave is sent back to the operator through the same or another communication channel. The control problem in this case is more challenging due to the fact that the master and slave manipulators are coupled by a control algorithm implemented in the software.

Long distances or communication media such as Internet can lead to time-delayed responses of the slave manipulator to the commands sent by the operator. Furthermore, the sensor data sent from the slave can also be delayed, which can lead to delayed corrective actions of the operator. The time-delays can hamper the performance of teleoperations or even destabilize the complete system. One of the early studies on the performance of telerobotic systems is conducted by Sheridan and Farrell, in [3]. They have found out that whenever the communication loop features time-delays, the operator adopts a move and wait strategy from which it can be deduced that the task completion time is linear with respect to the induced time-delay in the loop. A comparative study on teleoperation control schemes in the presence of time delays is performed by Arcara et. al. [4]. That comparison consideres five different aspects: stability as a function of time delay, perceived inertia and damping in free motion, position tracking performance, perceived stiffness in the case of interaction with a structured environment, and position drift between master and slave manipulators.

Among many available approaches, a popular remedy for time-delays is application of Smith predictors in the control structure. The main purpose of a Smith predictor is to render the control system time-delay free. An overview of Smith predictor type control architectures for time-delayed teleoperations is given in [5]. There, a force-position type predictive control architecture is proposed which combines two neural networks to online estimate and map the slave and environment dynamics at the master side. A nonlinear extension of the Smith predictor is developed by Wong et. al. in [6]. In [7], a time-delay compensation is applied to control systems with nonlinear dynamics and process dead-time. Normay-Rico et. al. give a broad review of dead-time compensators in [8], where they analyse the basic Smith predictor and propose design of suitable dead-time compensators for unstable systems. Scattering (or wave variables) is another common technique which aims to passify the communication channel. In [9], Miyoshi et. al. modified the approach by introducing wave filters in the scattering variables, designed by H_∞ method.

It is pointed out by Matijević et. al., in [10] that Smith predictor type control architectures are characterized by limited robustness and disturbance rejection capabilities. A new control architecture for systems with Smith predictors is proposed by Stojić et. al. to improve their robustness and performance of disturbance rejection. This architecture is based on the internal model principle and control together (IMPACT) approach. This approach is first proposed in [11], as a way to combine the internal model principle (IMP) and internal model control (IMC). The former (IMP) is used to cope with the disturbances that affect the plant, and is also known as the absorption principle. The latter (IMC) includes a nominal model of the plant in the controller structure in order to incorporate modeling uncertainty into the control system. Therefore, the IMPACT structure provides a systematic and intuitive way to separate the problems of predictor design and the disturbance rejection.

There exist different types of control architectures in bilateral teleoperation systems. These can be categorized based

This work is done in the frame of the Remote Robotics project funded from a Pieken in de Delta grant of the Dutch Ministry of Economy.

A. Denasi, D. Kostić and H. Nijmeijer are with Dynamics and Control Group, Department of Mechanical Engineering, Technische Universiteit Eindhoven, 5600 MB Eindhoven, The Netherlands. (e-mail: a.denasi@tue.nl, d.kostic@tue.nl, h.nijmeijer@tue.nl)

on the exchanged sensory information between the master and slave manipulators. Among these, the most common are position error (PERR) based, force error based and 4-channel control architectures.

In this paper, we address time-delay compensation and disturbance rejection in position error (PERR) based bilateral teleoperation. We employ the benefits of the IMPACT structure for this purpose. These are robustness against uncertainties and external disturbances. The problem is approached from a more engineering perspective. A more generic framework is utilized to model the master and slave manipulators by means of a feedback connection of a linear dynamical system and a nonlinear element. By doing so, incorporating nonlinear compensators into the local feedback controllers is possible. This allows us to deal with some practical issues such as friction or gravity compensation. Furthermore, a pragmatic rational is applied in the design of local controllers which is based on frequency response function (FRF) measurements and a pole placement method. Keeping the number of design parameters small, leads to an easy and straightforward way of tuning. The robust stability of the designed controller is analysed by means of the Nyquist criterion. The effectiveness of the approach is demonstrated through extensive experimentation. Preliminary results of this work are contained in [12].

This paper is organized as follows. In the next section, we present mathematical definitions to be used in the following sections of the paper. We introduce the problem of PERR based bilateral teleoperations together with a friction compensation scheme in Section III. In Section IV, we propose a time-delay compensation scheme for the PERR based bilateral teleoperations using the Smith predictor structure and an application of the IMPACT approach to increase the robustness, disturbance rejection and trajectory tracking performance. Simulation results are given in Section V-B. In Section V-C, illustrative experimental results are given. The conclusions and final remarks are given in Section VI.

II. MATHEMATICAL PRELIMINARIES

In what follows, the mathematical formulation of the problem is given in Laplace domain. In order to deal with certain type of nonlinearities, we consider the master/slave robots as Lur'e type of systems in this work. This means that they can be seen as a feedback interconnection of a linear dynamical system and a nonlinear memoryless element [13], as shown in Fig. 1, where $G(s)$ represents the transfer function of the

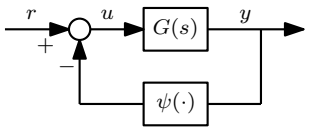

Fig. 1. Feedback connection of a linear dynamical system and a nonlinear element.

linear dynamical system and $\psi(\cdot)$ is a memoryless, possibly time-varying, nonlinearity, which is piecewise continuous in time and locally Lipschitz in the output y. A similar type of modeling approach which takes into account several sources of nonlinearities was also used in [14].

III. POSITION ERROR BASED TELEOPERATIONS

In a PERR based teleoperation scenario, the slave manipulator, being subject to modeling uncertainties and disturbances, is required to realize the commands sent from the master device handled by the operator. Only the position information is exchanged between the master and slave manipulators as presented in Fig. 2 [1]. In the given figure, $G_m(s)$ and $G_s(s)$ denote transfer functions of the master and slave manipulators, respectively. Here, $\varphi_m(\cdot)$, $\varphi_s(\cdot)$ are the nonlinear terms such as friction or cogging torques/forces and $\hat{\varphi}_m(\cdot)$, $\hat{\varphi}_s(\cdot)$ are the suitable nonlinear compensation torques/forces for the master and slave manipulators, respectively. The control laws for the master and slave manipulators are given by

$$\begin{aligned} U_m(s) = K_{m,1}(s)(Q_{ref}(s) - Q_m(s)) \\ + K_{m,2}(s)(Q_s(s)e^{-T_d s} - Q_m(s)), \end{aligned} \tag{1}$$

$$U_s(s) = K_s(s)(Q_m(s)e^{-T_d s} - Q_s(s)), \tag{2}$$

where $K_{m,1}(s)$, $K_{m,2}(s)$ and $K_s(s)$ are the local controllers for the master/slave manipulators, respectively, $Q_m(s)$ is position of the master, $Q_s(s)$ is the slave position, and T_d represents the time delay in the communication channel.

Remark 1: It should be mentioned that, in (1) using two different control laws for the two different kind of errors, $Q_{ref}(s) - Q_m(s)$ and $Q_s(s)e^{-T_d s} - Q_m(s)$, provides extra degrees of freedom for tuning and higher performance, eventually. Keeping that in mind, we should emphasize that, for the sake of easy tuning, the local controllers $K_{m,1}(s)$ and $K_{m,2}(s)$ are selected identical to each other (i.e. $K_{m,1}(s) = K_{m,2}(s) = K_m(s)$). Therefore, the design and stability analysis of the teleoperated system is performed for the case $K_{m,1}(s) = K_{m,2}(s) = K_m(s)$.

In this work, single degree-of-freedom manipulators are considered at the master and slave sides. Furthermore, the nonlinear terms which we are interested in, are related to the friction torques/forces. The dynamics of these manipulators in time domain, that apply as they conduct free motions, are given by

$$J_m\ddot{q}_m + \tau_{f,m}(\dot{q}_m) + C_m q_m = \tau_m, \tag{3}$$

$$J_s\ddot{q}_s + \tau_{f,s}(\dot{q}_s) + C_s q_s = \tau_s, \tag{4}$$

where J_m, $\tau_{f,m}(\dot{q}_m)$, C_m and J_s, $\tau_{f,s}(\dot{q}_s)$, C_s are the masses (for translational dynamics)/mass moments of inertia (for rotational dynamics), the friction forces/torques and the spring coefficient of the master and slave manipulators, respectively, while τ_m and τ_s are the input forces/torques. Appropriate parameters and their respective units are selected depending on whether the dynamics is translational or rotational.

There are many different models in the literature to represent the friction phenomena that exist in robotic systems [15]. The complexity of these models depends on the velocity regime at which the system operates. In this work, we concentrate on a relatively simple friction model which is comprised of Coulomb friction and viscous friction terms:

$$\tau_{f,m}(\dot{q}_m) = \tau_{c,m}\mathrm{sgn}(\dot{q}_m) + B_m\dot{q}_m, \tag{5}$$

$$\tau_{f,s}(\dot{q}_s) = \tau_{c,s}\mathrm{sgn}(\dot{q}_s) + B_s\dot{q}_s, \tag{6}$$

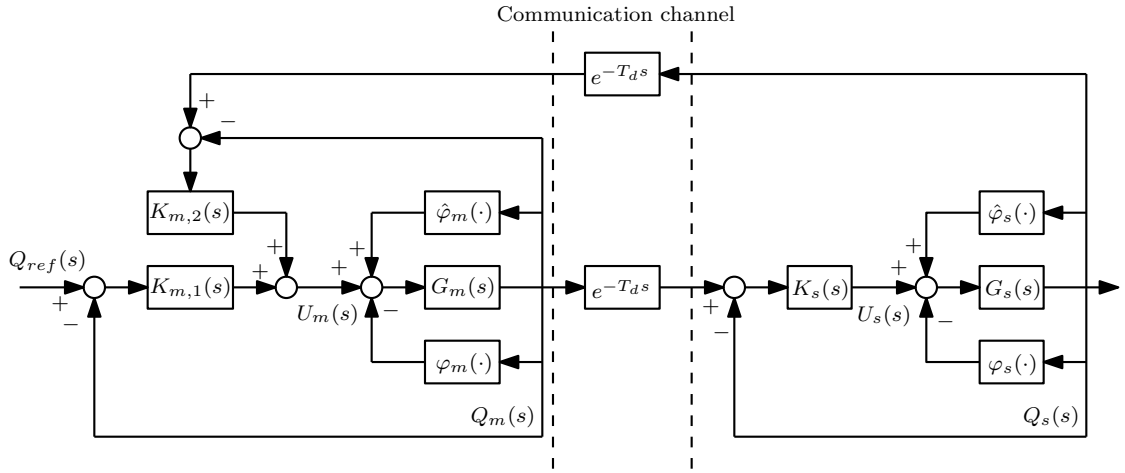

Fig. 2. Position error based teleoperation scheme.

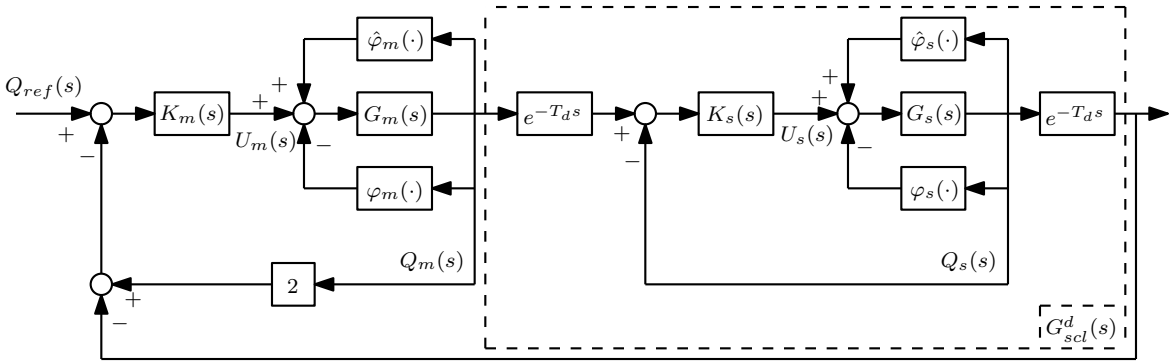

Fig. 3. Position error based teleoperation scheme redrawn.

where $\text{sgn}(\cdot)$ is the signum function and $\tau_{c,m}$, B_m and $\tau_{c,s}$, B_s are the Coulomb friction and viscous friction coefficients of the master and slave manipulators, respectively. The effect of the Coulomb friction can be compensated by using Coulomb friction compensation, if the inputs to the master and slave robots are taken as,

$$\tau_m = \hat{\tau}_{c,m}\text{sgn}\left(\dot{q}_m\right) + u_m, \tag{7}$$

$$\tau_s = \hat{\tau}_{c,s}\text{sgn}\left(\dot{q}_s\right) + u_s, \tag{8}$$

where $\hat{\tau}_{c,m}$, $\hat{\tau}_{c,s}$ are Coulomb friction compensation coefficients and u_m, u_s are the new control inputs. These new control inputs can be used to design suitable control laws such as (1) and (2). From (3), (4), (5) and (6), we can determine the transfer functions of two manipulators as

$$G_m(s) = \frac{1}{J_m s^2 + B_m s + C_m}, \tag{9}$$

$$G_s(s) = \frac{1}{J_s s^2 + B_s s + C_s}. \tag{10}$$

In the following, we will assume that the effect of Coulomb friction is exactly compensated.

IV. INTERNAL MODEL PRINCIPLE AND CONTROL TOGETHER

A. Control Structure

This section describes an IMPACT structure which is suitable for the considered PERR teleoperation problem. The block diagram of the IMPACT structure is shown in Fig. 4. Here, D denotes a disturbance at the slave side of the telemanipulation system, such as undesired vibrations acting at the output of the slave manipulator. The structure shown in Fig. 4 implements a Smith predictor at the master side, while at the slave side $\tilde{G}^d_{scl}$ is the internal nominal plant model and $A(s)/C(s)$ is the transfer function representing an internal model of the disturbances. The difference between the outputs of the actual and nominal plants are filtered by the transfer function $(1/R(s))(A(s)/C(s))$, where $R(s)$ is a transfer function in the disturbance estimator whose design will be introduced in the next section. The resulting signal $\hat{D}$ is the disturbance estimator. The nominal plant model is given by

$$\tilde{G}^d_{scl}(s) = \frac{K_s(s)\tilde{G}_s(s)}{1 + K_s(s)\tilde{G}_s(s)} e^{-2Ls}, \tag{11}$$

where $\tilde{G}_s(s)$ is the nominal model of the slave manipulator and L is the nominal value of the time-delay T_d in a single direction of the communication channel. In our control design,

the nominal value L is considered to be constant, known and same for both forward and backward directions; it can be determined by practical measurements, as an average of the actual time-delays. Since T_d is known upto a certain degree of accuracy, the effect of the mismatch between T_d and L can be investigated via robustness analysis. The actual plant is given by,

$$G^d_{scl}(s) = \frac{K_s(s)G_s(s)}{1 + K_s(s)G_s(s)} e^{-2T_d s}, \tag{12}$$

where $G_s(s)$ represents the actual transfer function of the slave manipulator.

B. Controller Design

This section presents designs of the local controllers for the master and slave manipulators and describes a method for disturbance absorption. Following the rationale given in [7], the local feedback controllers $K_m(s)$ and $K_s(s)$ for the master and slave manipulators, respectively, are designed based on the inverse plant model

$$K_m(s) = \frac{1}{W(s) - 1} \frac{1}{\tilde{G}_m(s)}, \tag{13}$$

$$K_s(s) = \frac{1}{W(s) - 1} \frac{1}{\tilde{G}_s(s)}, \tag{14}$$

where $\tilde{G}_m(s)$ and $\tilde{G}_s(s)$ are the nominal models of the master and slave manipulators, respectively, and $W(s)$ is the characteristic polynomial describing the desired location of the closed-loop poles for the local feedback loops at the master and slave sides

$$W(s) = (\epsilon s + 1)^r. \tag{15}$$

Here, $\epsilon > 0$ and r is the relative order of the nominal models of the master and slave manipulators. Polynomial (15) is selected such as to keep the number of tuning parameters small. We assume that the dynamics of the master and slave manipulators described by (9) and (10) are known and given by

$$\tilde{G}_m(s) = \frac{1}{\tilde{J}_m s^2 + \tilde{B}_m s + \tilde{C}_m}, \tag{16}$$

$$\tilde{G}_s(s) = \frac{1}{\tilde{J}_s s^2 + \tilde{B}_s s + \tilde{C}_s}, \tag{17}$$

where $\tilde{J}_m$, $\tilde{J}_s$, $\tilde{B}_m$, $\tilde{B}_s$, $\tilde{C}_m$ and $\tilde{C}_s$ are the nominal model parameters that are determined, for instance, using system identification. For the manipulator dynamics of the second order, r equals to 2 in (15).

Remark 2: The local control laws (13) and (14) may or may not have integral action depending on the nominal master/slave manipulator models (16)-(17). For example, when the nominal models do not have stiffness terms (i.e. $\tilde{C}_m = \tilde{C}_s = 0$), the local control laws can be written as,

$$K_m(s) = \frac{\tilde{J}_m s + \tilde{B}_m}{\epsilon^2 s + 2\epsilon},$$
$$K_s(s) = \frac{\tilde{J}_s s + \tilde{B}_s}{\epsilon^2 s + 2\epsilon} \tag{18}$$

which are of lead or lag type depending on the location of their poles/zeros. In the case when the stiffness terms of the nominal models are nonzero (i.e. $\tilde{C}_m \neq 0$ and $\tilde{C}_s \neq 0$), we obtain the following local control laws,

$$K_m(s) = \frac{\tilde{J}_m s^2 + \tilde{B}_m s + \tilde{C}_m}{s\left(\epsilon^2 s + 2\epsilon\right)},$$
$$K_s(s) = \frac{\tilde{J}_s s^2 + \tilde{B}_s s + \tilde{C}_s}{s\left(\epsilon^2 s + 2\epsilon\right)} \tag{19}$$

which have an integral action in their structure.

In addition to the feedback controllers (13) and (14), the tracking performance can be improved by adding the feedforward terms related to the velocity and acceleration profiles of the reference trajectory for the master manipulator. From (11), (14) and (15), the nominal plant model is given by

$$\tilde{G}^d_{scl}(s) = \frac{1}{(\epsilon s + 1)^2} e^{-2Ls}. \tag{20}$$

Referring to Fig. 4, we can determine the closed-loop transfer functions, based on the nominal plant between the inputs $Q^d_{ref}(s)$ and $D(s)$ and the output $Q_s(s)$:

$$N(s) = \frac{Q_s(s)}{Q^d_{ref}(s)} = \frac{K_m(s)\tilde{G}_m(s)K_s(s)\tilde{G}_s(s)}{\zeta(s) + K_m(s)\tilde{G}_m(s)}, \tag{21}$$

$$\frac{Q_s(s)}{D(s)} = \left(1 + N(s)e^{-2Ls}\right)\left(\frac{1}{1 + K_s(s)\tilde{G}_s(s)}\right) \times \left(1 - \frac{A(s)}{R(s)C(s)} \frac{K_s(s)\tilde{G}_s(s)e^{-2Ls}}{1 + K_s(s)\tilde{G}_s(s)}\right), \tag{22}$$

with

$$\zeta(s) = \left(1 + K_s(s)\tilde{G}_s(s)\right)\left(1 + K_m(s)\tilde{G}_m(s)\right)$$

where $Q^d_{ref}(s) = Q_{ref}(s)e^{-Ls}$ represents the delayed reference signal. When (13)-(15) and (16)-(17) are substituted into (21) and (22), we obtain:

$$N(s) = \frac{Q_s(s)}{Q^d_{ref}(s)} = \frac{1}{\epsilon^4 s^4 + 4\epsilon^3 s^3 + 7\epsilon^2 s^2 + 6\epsilon s + 1}, \tag{23}$$

$$\frac{Q_s(s)}{D(s)} = \left(1 + N(s)e^{-2Ls}\right)\left(\frac{\epsilon s(\epsilon s + 2)}{(\epsilon s + 1)^2}\right) \times \left(1 - \frac{A(s)}{R(s)C(s)} \frac{e^{-2Ls}}{(\epsilon s + 1)^2}\right). \tag{24}$$

The stability of the closed-loop system described by the transfer function (23) can be evaluated using the Routh's stability criterion [16]. It can be shown that the elements in the first column of the Routh's table are positive, since by definition, $\epsilon > 0$. According to the Routh criterion, this implies that the poles of the closed-loop are all in the left half of the complex plane.

By applying the final value theorem to (24), it can be shown that the effect of the disturbance D on the steady-state motion

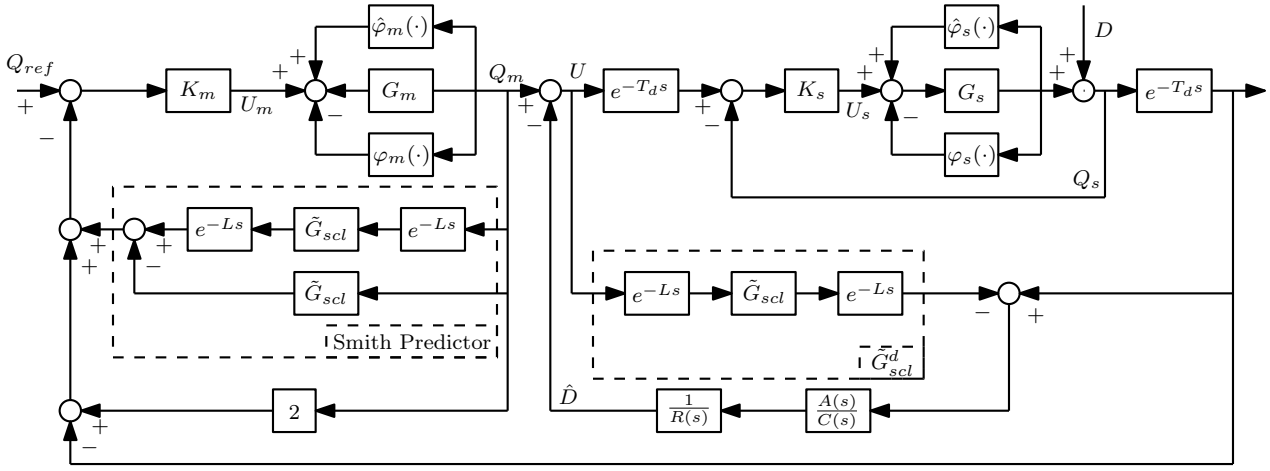

Fig. 4. IMPACT structure for PERR based teleoperation system.

of the slave manipulator diminishes if

$$\lim_{s\to 0} s\left(s\left(1+N(s)e^{-2Ls}\right)s\left(\frac{\epsilon(\epsilon s+2)}{(\epsilon s+1)^2}\right)\times\left(1-\frac{A(s)}{R(s)C(s)}\frac{e^{-2Ls}}{(\epsilon s+1)^2}\right)D(s)\right)=0. \quad (25)$$

Since

$$\lim_{s\to 0}\left(1+N(s)e^{-2Ls}\right)=2,\ \lim_{s\to 0}\left(\frac{\epsilon(\epsilon s+2)}{(\epsilon s+1)^2}\right)=2\epsilon, \quad (26)$$

to have (25) achieved, the following should hold:

$$\lim_{s\to 0} s^2\left(1-\frac{A(s)}{R(s)C(s)}\frac{e^{-2Ls}}{(\epsilon s+1)^2}\right)D(s)=0. \quad (27)$$

The polynomial $A(s)$ can be selected as any stable polynomial. Here it is selected as

$$A(s)=(\epsilon s+1)^2 A_0(s), \quad (28)$$

where $A_0(s)$ is a polynomial which is determined based on the disturbance. To guarantee stability of the disturbance estimator, polynomials $R(s)$ and $C(s)$ should have stable zeros. A simple way to select $R(s)$ and $C(s)$, which decreases the number adjustable parameters, is proposed in [17]:

$$R(s)=1, \qquad C(s)=(T_0 s+1)^n, \quad (29)$$

where T_0 is a time constant and n is an order of the filter. The design parameters T_0 and n determine the speed of the disturbance absorption process. The disturbance is absorbed more quickly if lower values are selected for T_0 and n. For the particular choice of (28) and (29), condition (27) can be rewritten as,

$$\lim_{s\to 0} s^2\left(C(s)-A_0(s)e^{-2Ls}\right)D(s)=0. \quad (30)$$

It can be realized from (30) that the absorption of a step disturbance (i.e. $D(s)=1/s$) can be achieved for any $A_0(s)$ and $C(s)$. For a class of polynomial disturbances $d(t)=\sum_{i=0}^{m} d_i t^i$, after application of the L'Hôpital rule, we can uniquely determine the polynomial $A_0(s)$ using the following expression,

$$\lim_{s\to 0}\frac{d^k}{ds^k}\left(C(s)-A_0(s)e^{-2Ls}\right)=0, \qquad 0\le k<m. \quad (31)$$

As an example, for a ramp disturbance (i.e. $D(s)=1/s^2$) by using (28) and (31) we obtain

$$A_0(0)=1, \quad \text{for } k=0. \quad (32)$$

In the case of a disturbance that can be represented as a second order function of time (i.e. $d(t)=t^2/2$, thus $D(s)=1/s^3$), we determine

$$A_0(0)=1 \quad \text{for } k=0, \quad (33)$$

$$A_0(s)=(nT_0+2L)s+A_0(0) \quad \text{for } k=1. \quad (34)$$

For an arbitrary disturbance described by its Laplace transform $D(s)=N_d(s)/D_d(s)$, such as a sinusoid function (i.e. $D(s)=1/(s^2+\omega^2)$ for $d(t)=\sin\omega t$), the following condition is induced from (30),

$$C(s)-A_0(s)e^{-2Ls}=\Phi(s)B(s), \quad (35)$$

where $\Phi(s)$ represents the absorption polynomial determined by $\Phi(s)\equiv D_d(s)$. In order to solve equation (35) for $A_0(s)$ which is used in the design of the disturbance estimator, the exponential term e^{-2Ls} can be approximated by the Taylor series expansion as

$$e^{-2Ls}\cong\sum_{k=0}^{N}\frac{(-2Ls)^k}{k!}, \quad (36)$$

with N being the number of terms used in the approximation and then substituted into (35) which leads to the Diophantine equation given by

$$A_0(s)\sum_{k=0}^{N}\frac{(-2Ls)^k}{k!}+B(s)\Phi(s)=C(s). \quad (37)$$

The obtained relation does not have a unique solution in terms of $A_0(s)$ (cf. [18]). A solution procedure for the Diophantine

equation is given in [19]. The only constraint is due to causality, i.e.

$$\deg(A(s)) = 2 + \deg(A_0(s)) \leq \deg(C(s)). \tag{38}$$

The solution procedure roughly works as follow. First select $C(s)$, N and the degree of the polynomials $A_0(s)$ and $B(s)$, and then substitute the corresponding absorption polynomial $\Phi(s)$ for the disturbance. After that, equation (37) can be solved for the polynomials $A_0(s)$ and $B(s)$, by equating the coefficients of the terms of equal order on both sides.

C. Robustness Analysis

Since the control design is based on the nominal plant model $\tilde{G}^d_{scl}(s)$, it should be investigated how uncertainties in the plant parameters and unmodeled dynamics influence stability and control performance of the considered teleoperated system. As the starting point of our robustness analysis, we assume that the real plant $G^d_{scl}(s)$ belongs to the set Π of plants that differ from the nominal plant up to an additive uncertainty. Mathematically, this set can be defined as follows

$$\Pi = \left\{ G^d_{scl} : \left| G^d_{scl}(j\omega) - \tilde{G}^d_{scl}(j\omega) \right| \leq \bar{l}_a(\omega) \right\}. \tag{39}$$

where $\bar{l}_a(\omega)$ is the worst-case bound on the additive uncertainty. Thus, each member of this set satisfies:

$$G^d_{scl}(j\omega) = \tilde{G}^d_{scl}(j\omega) + l_a(j\omega), \tag{40}$$

where $l_a(j\omega)$ is the additive uncertainty and $|l_a(j\omega)| \leq \bar{l}_a(\omega)$. According to [20], [18], in order to have all elements of the set Π stable, it is sufficient that,

$$|l_a(j\omega)| < \beta(\omega) \tag{41}$$

holds. Here, $\beta(\omega)$ is given by

$$\beta(\omega) = \left| \frac{\tilde{G}^d_{scl}(j\omega)}{G_{cl,des}(j\omega)} \right| \left| \frac{G_{ff}(j\omega)}{G_{fb}(j\omega)} \right|, \tag{42}$$

where $G_{cl,des}(s)$ represents the desired closed-loop transfer function given by (23), while $G_{ff}(s)$ and $G_{fb}(s)$ are defined by

$$U(s) = G_{ff}(s)Q_{ref}(s) - G_{fb}(s)Q_s(s), \tag{43}$$

where the transfer functions $G_{ff}(s)$ and $G_{fb}(s)$ represent the feedforward and feedback parts of the overall control structure, respectively. The robust stability condition (41) can be derived by rewriting the overall control structure in a more compact form and then employing the Nyquist stability criterion. The overall control structure can be derived using (15), (28) and (29) as,

$$U(s) = \frac{(\epsilon s+1)^2 C(s)}{C(s) - A_0(s)e^{-2Ls}} \left[\frac{1}{\Gamma(s) + e^{-2Ls}} Q_{ref}(s) + \frac{C(s) - A_0(s)\left(\Gamma(s) + e^{-2Ls}\right)}{C(s)\left(\Gamma(s) + e^{-2Ls}\right)} Q_s(s) e^{-Ls} \right] \tag{44}$$

with

$$\Gamma(s) = (\epsilon s + 1)^4 + \epsilon s (\epsilon s + 2).$$

By using (15), (28) and (29), the robust stability bound (42) can be rewritten as

$$\beta(\omega) = \left| \frac{\Gamma(j\omega)}{(\epsilon j\omega + 1)^2} \right| \times \left| \frac{C(j\omega)}{C(j\omega) - A_0(j\omega)\left(\Gamma(j\omega) + e^{-2Lj\omega}\right)} \right| \tag{45}$$

with

$$\Gamma(j\omega) = (\epsilon j\omega + 1)^4 + \epsilon j\omega (\epsilon j\omega + 2).$$

Inclusion of the disturbance estimator within the IMPACT structure can increase robustness of the system to uncertainties in the plant parameters. At high frequencies, $\beta(\omega)$ converges to a constant value if $\deg C(s) = \deg A(s) = 2 + \deg A_0(s)$. This can be shown by selecting $C(s) = (T_0 s + 1)^n$ and $A_0(s) = a_{n-2}s^{n-2} + a_{n-3}s^{n-3} + \cdots + a_1 s + a_0$, since

$$\lim_{\omega \to \infty} \beta(\omega) = \frac{T_0^n}{\epsilon^2 a_{n-2}}. \tag{46}$$

In the case when $\deg C(s) > \deg A(s)$, $\beta(\omega)$ goes to infinity at high frequencies, i.e.

$$\lim_{\omega \to \infty} \beta(\omega) \to \infty. \tag{47}$$

Another observation is that selecting a lower value for ϵ, in order to reduce the transient in setpoint tracking, reduces the robustness of the system. Thus, there exists a tradeoff between performance and robustness.

V. NUMERICAL AND EXPERIMENTAL ANALYSIS

In this section, our experimental setup is introduced. Then, simulation results based on identified system models are given. Finally, experimental results are presented.

A. Experimental Setup

The experiments are conducted on two similar five degree-of-freedom manipulators, fabricated by the Centre for Manufacturing Technology (CFT) Philips Laboratory. The experimental setup that is used in the experiments is shown in Fig. 5 with its schematic representation shown in Fig. 6, respectively. During the experiments, the horizontal degree-of-freedom marked with number 1, shown in Fig. 6, is used in both manipulators. Two manipulators are connected to the same PC via ethernet connection and control software is implemented in Matlab/Simulink 2006a. The sampling frequency of the controller is 500 Hz. The time delay T_d due to communication between the master and slave robots is emulated in software. In all experiments, the following smooth Coulomb friction compensation law is used,

$$\tau_m = \hat{\tau}_{c,m} \tanh(\alpha_m \dot{q}_m) + u_m, \tag{48}$$

$$\tau_s = \hat{\tau}_{c,s} \tanh(\alpha_s \dot{q}_s) + u_s, \tag{49}$$

for the master and slave robots respectively. The Coulomb friction compensation coefficients, obtained by means of an empirical estimation procedure, are $\alpha_m = \alpha_s = 50$, $\hat{\tau}_{c,m} = 1$ and $\hat{\tau}_{c,s} = 0.6$ for the master and slave robots, respectively [15]. The nominal transfer functions, $\tilde{G}_m(s)$ and $\tilde{G}_s(s)$ for

Fig. 5. Philips CFT robot.

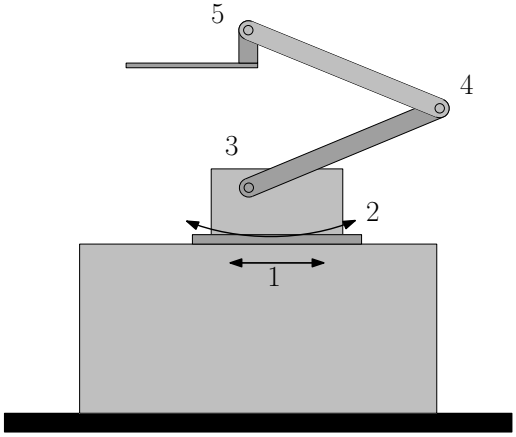

Fig. 6. Schematic representation of Philips CFT robot.

TABLE I
PARAMETERS USED IN SIMULATIONS

Parameter	Master	Slave
Sampling time [s]	0.002	
Real mass, J_m & J_s [kg]	15.601	9.871
Modeled mass, $\tilde{J}_m$ & $\tilde{J}_s$ [kg]	7.801	4.935
Real viscous friction, B_m & B_s [kg/s]	15.673	2.295
Modeled viscous friction, $\tilde{B}_m$ & $\tilde{B}_s$ [kg/s]	23.51	3.443

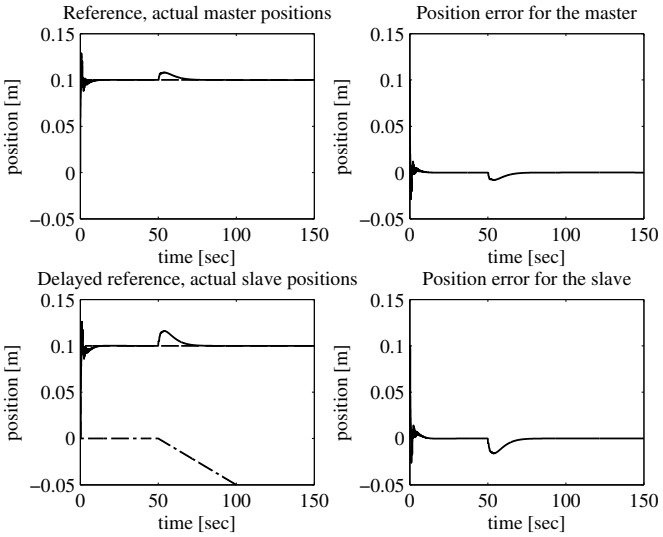

Fig. 7. Results for disturbance absorption of a ramp disturbance. Reference (- -) and actual (–) master angles are shown in the upper left part of the figure. Delayed reference (- -), actual slave (–) angles and the disturbance (– · –) are shown in the lower left part.

the master and slave robots, respectively, are obtained using frequency response function (FRF) measurements, with a multisine excitation signal [21]. For simplicity, we consider only inertia and viscous friction terms for the nominal manipulator dynamics. Therefore, the following second order transfer functions are fitted to the frequency response measurements of the master and slave manipulators,

$$\tilde{G}_m(s) = \frac{0.0641}{s^2 + 1.005s} = \frac{1}{15.601s^2 + 15.673s}, \quad (50)$$

$$\tilde{G}_s(s) = \frac{0.1013}{s^2 + 0.2325s} = \frac{1}{9.871s^2 + 2.295s} \quad (51)$$

respectively. In all experiments, the local control laws are designed in continuous time using (13)-(14) and then discretized using Tustin approximation. Furthermore, the tuning of the control laws is performed for the optimal tracking error performance.

B. Illustrative Simulations

In this section we present results of a simulation case-study which illustrates application of the proposed IMPACT structure to the PERR based bilateral teleoperation problem. First, the absorption of a ramp type of disturbance is considered. Then, robustness of the system dynamics against parametric uncertainties is analysed. The master and slave models that are used during the simulations are given by the transfer functions (50) and (51), respectively. The parameters of the master and slave manipulators are given in Table I. These parameters are obtained by fitting (16) and (17) to the transfer functions (50) and (51). For simplicity, in simulations we consider only inertia and viscous friction terms in both the real and nominal manipulator dynamics. The modeled values of the inertias and viscous friction coefficients correspond to 50% level of uncertainty.

The first case-study is related to absorption of a ramp disturbance. The corresponding results are shown in Fig. 7. In this simulation, the reference is a step-function $q_{ref}(t) = h(t)$, defined as,

$$h(t) = \begin{cases} 0.1, & t \geq 0 \\ 0, & t < 0 \end{cases}. \quad (52)$$

The two plots at the top of this figure show the reference q_{ref}, position q_m of the master manipulator, and the difference (error) between them. The position q_s of the slave manipulator, the reference delayed by T_d, and the scaled disturbance (with a scaling factor of 0.01, being scaled for the ease of plotting) are shown in the two plots at the bottom of Fig. 7. The disturbance absorption polynomial is selected as $A_0(s) = 1$ and the lowpass filter parameters are $n = 3$ and $T_0 = 2$. The main controller parameter is selected as $\varepsilon = 0.045$. The actual time delay is $T_d = 0.25$ [s] and the modeled time-delay is $L = 0.3125$ [s] corresponding to an uncertainty of 25%. It can be observed from Fig. 7 that the influence of the disturbance is

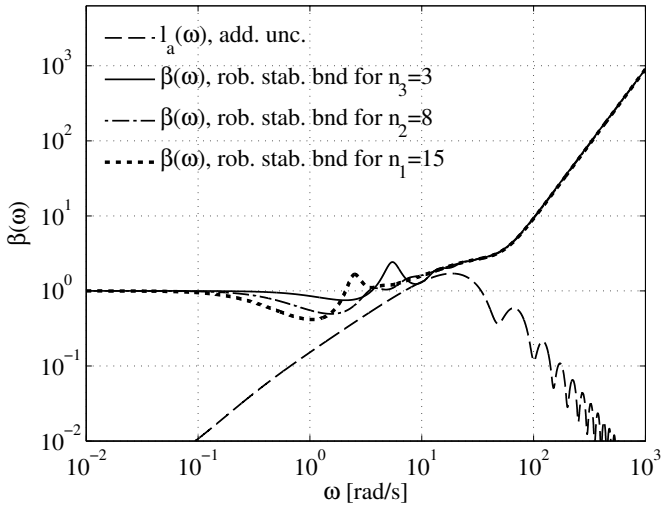

Fig. 8. Robustness analysis for different n values.

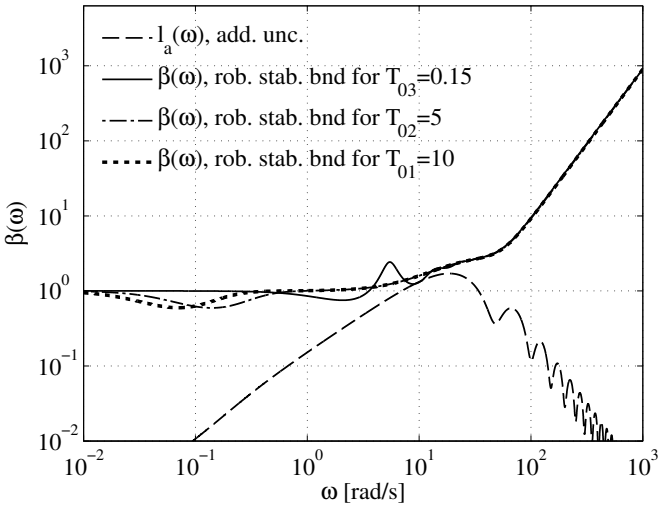

Fig. 9. Robustness analysis for different T_0 values.

absorbed reasonably fast and that the steady-state value of the output remains the same as before the disturbance is applied. Furthermore, it can be observed that the master-manipulator is also affected by the disturbance, however its influence vanishes after the transients. Smaller values for ϵ, n and T_0 can be selected to improve the control performance, however at the cost of decreasing the robust stability.

In Figs. 8 and 9, we show results of the robustness analysis when the disturbance absorption polynomial is $A_0(s) = 1$. The main controller parameter is selected as $\epsilon = 0.03$. The modeled and actual time delays are the same as in the previous case. The additive uncertainty bounds $|l_a(j\omega)|$ together with the robust stability bounds $\beta(\omega)$ are depicted in these figures. The robust stability bounds are plotted in Fig. 8 for $T_0 = 0.15$ and for three values of n: $(n_1, n_2, n_3) = (15, 8, 3)$. It can be observed from this figure that the robustness of the system improves if n is increased. The robust stability bounds are plotted in Fig. 9 for $n = 3$ and for three values of T_0: $(T_{01}, T_{02}, T_{03}) = (10, 5, 0.15)$. It can be observed from this figure that the robustness of the system improves for higher values of T_0. The fluctuations observed in Figs. 8 and 9 at frequencies higher than $\omega = 100$ rad/s are caused by the mismatch between the real and nominal values of the time-delay.

C. Experimental Results

In this section, first experimental results demonstrating the tracking error performance of the local controllers are given. Then, tracking performance in the case of bilateral teleoperations is presented. Finally, robustness of the IMPACT structure to uncertainties in time-delay and its disturbance rejection performance are shown. A repetitive second order reference trajectory, which takes approximately 6 seconds, is used during the tracking experiments whose details are given in the Appendix A. The individual tracking error performance of each manipulator for the local control laws given by (13)-(14) is shown in Fig. 10. The local controller parameter for this experiment is selected as $\epsilon = 0.04$. It can be noticed from this

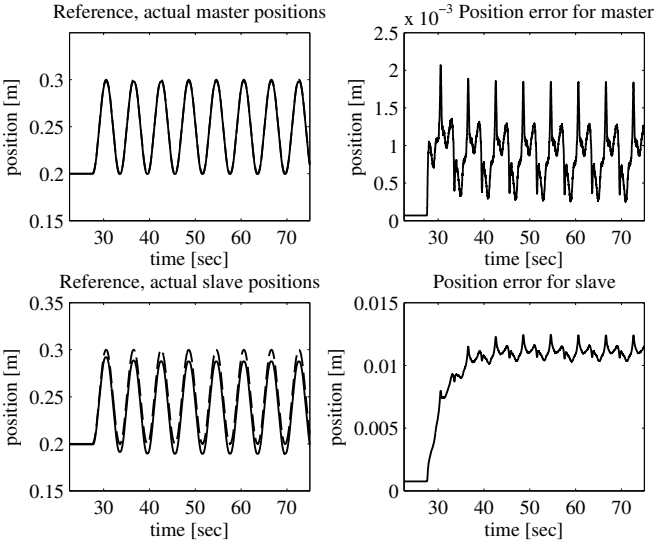

Fig. 10. Individual tracking performance of master and slave manipulators using the local control laws. Reference (- -) and actual (–) master and slave positions.

figure that the steady state errors remain for both the master and slave robots, since the local controllers are only of the lead filter type with no integral action included. The absence of the integral action in the local control laws can be realized when the fitted transfer functions of the master and slave robots (50) and (51), respectively, are inspected according to the Remark 2.

The results related to the case when no IMPACT structure is applied and without time-delay ($T_d = 0$), are shown in Fig. 11. In this experiment, the teleoperation scheme shown in Fig. 3 is implemented with only local controllers given by equation (13). The local controller parameter for this experiment is $\varepsilon = 0.045$. It can be observed from Fig. 11 that, even when time-delays are not present in the teleoperated system, an offset is present in the tracking errors and now also affecting the master. The results when IMPACT structure is not applied and

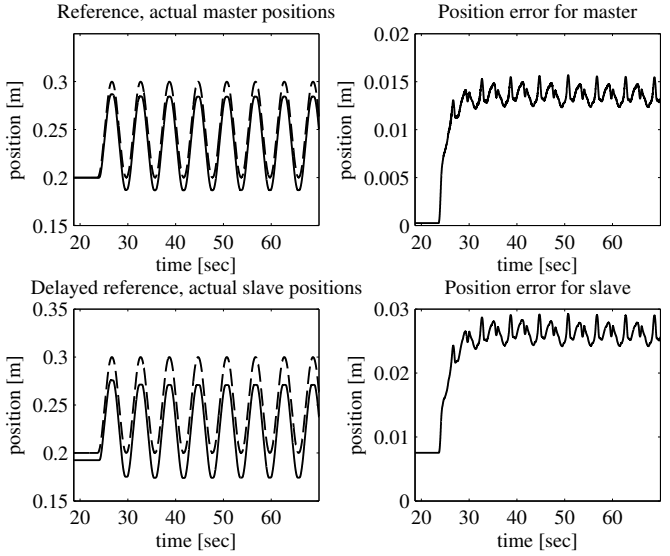

Fig. 11. Results for bilateral teleoperation without the IMPACT structure and without any time-delay. Reference (- -) and actual (–) master positions are shown in the upper left part of the figure. Delayed reference (- -), actual slave (–) positions are shown in the lower left part.

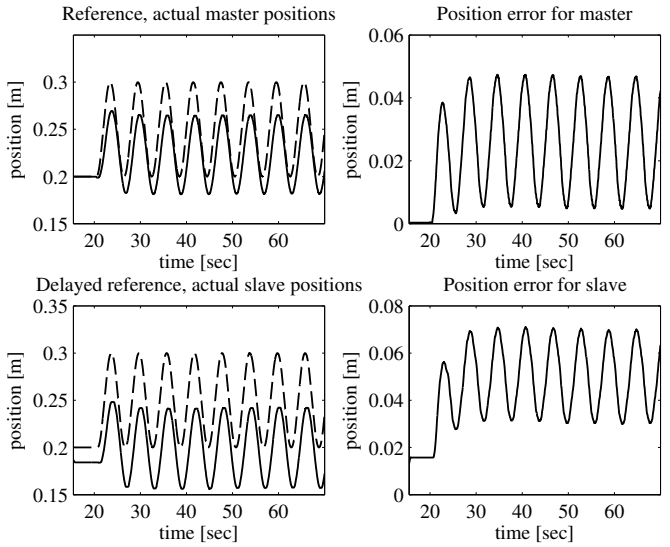

Fig. 12. Results for bilateral teleoperation without the IMPACT structure for 0.25 second time delay. Reference (- -) and actual (–) master positions are shown in the upper left part of the figure. Delayed reference (- -), actual slave (–) positions are shown in the lower left part.

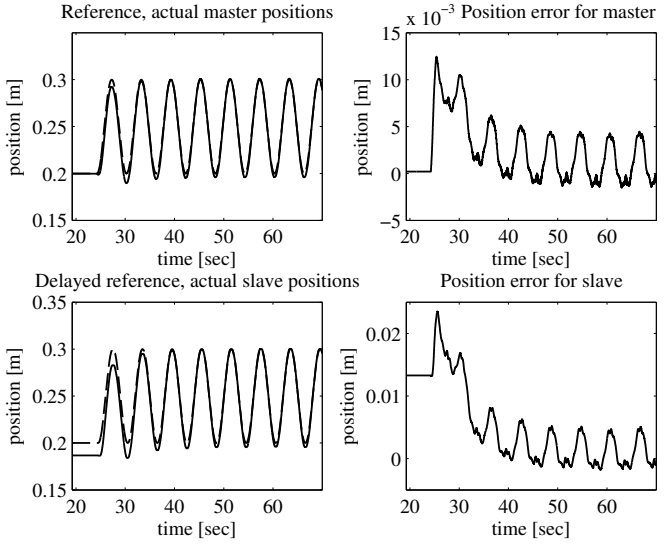

Fig. 13. Results for bilateral teleoperation with the IMPACT structure with $T_d = 0.25$ seconds. Reference (- -) and actual (–) master positions are shown in the upper left part of the figure. Delayed reference (- -), actual slave (–) positions are shown in the lower left part.

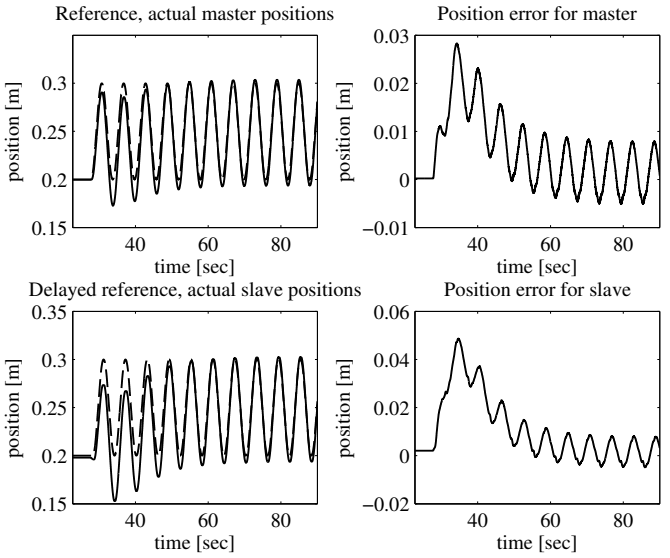

Fig. 14. Results for bilateral teleoperation with the IMPACT structure with $T_d = 0.5$ seconds. Reference (- -) and actual (–) master positions are shown in the upper left part of the figure. Delayed reference (- -), actual slave (–) positions are shown in the lower left part.

a time-delay of $T_d = 0.25$ seconds is emulated, are shown in Fig. 12. The local controller parameter for this experiment is $\varepsilon = 0.09$. It can be observed that the position errors of both master and slave manipulators are quite high (at the level of 50%) and fluctuate around a non-zero value.

The results when the IMPACT structure is applied are presented in Fig. 13, with the local controller parameter, $\varepsilon = 0.045$. The parameters of the lowpass filter $C(s)$ are selected as $T_0 = 2$ and $n = 3$. It can be observed that the offset in the error, which can be thought as a constant output disturbance, is mostly reduced and the tracking error is significantly improved (the maximum after the transient vanishes, is below 5%). The remaining peaks in the error occur when the position signal changes direction, which can be due to imperfect cancellation of friction at low velocities. The results with the IMPACT structure when a time-delay of $T_d = 0.5$ seconds is introduced, are shown in Fig. 14. For this experiment, the values of the parameters of the local control laws and the low-pass filter $C(s)$ are, $\varepsilon = 0.0535$, $T_0 = 3$ and $n = 3$, respectively.

Finally, the results with the IMPACT structure in situation when there are mismatches in time-delay and disturbances are presented. The results of the experiment for a virtual ramp disturbance acting at the output of the slave are shown

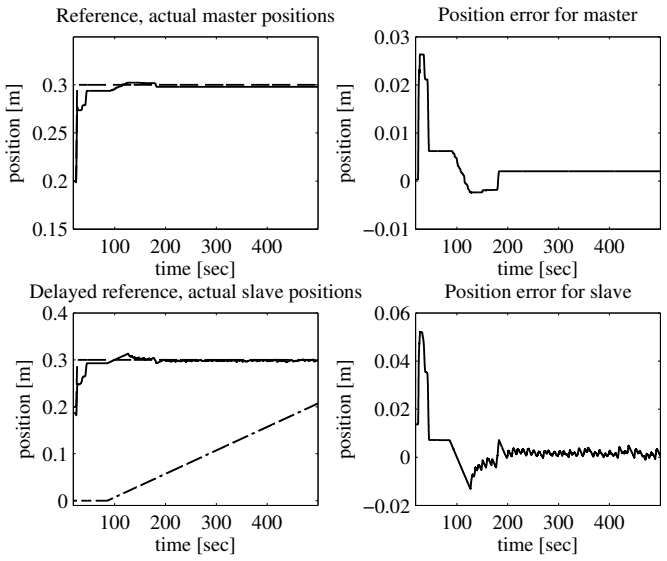

Fig. 15. Results for disturbance absorption of a ramp disturbance. Reference (- -) and actual (–) master positions are shown in the upper left part of the figure. Delayed reference (- -), actual slave (–) positions and the disturbance ($-\cdot-$) are shown in the lower left part.

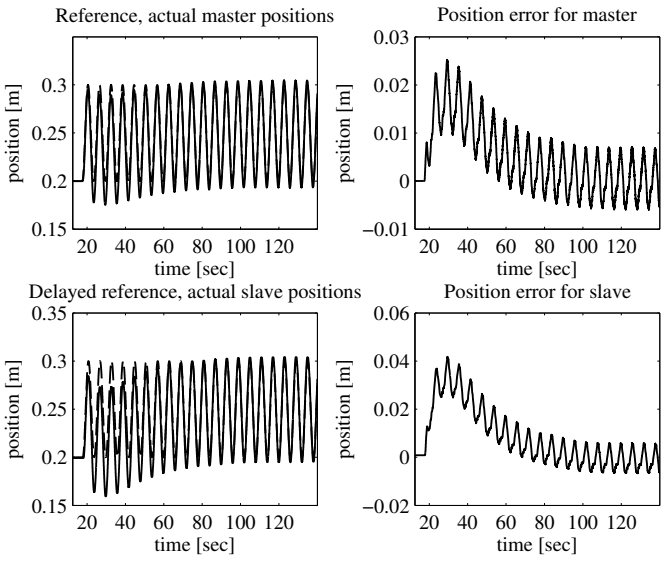

Fig. 16. Results for bilateral teleoperation with the IMPACT structure with $T_d = 0.25$ and $L = 0.275$ seconds. Reference (- -) and actual (–) master positions are shown in the upper left part of the figure. Delayed reference (- -), actual slave (–) positions are shown in the lower left part.

in Fig. 15. After the system is settled, approximately at 85 seconds, the disturbance is added to the output of the slave. The local controller parameter is selected as, $\varepsilon = 0.05$. The parameters of the lowpass filter $C(s)$ are selected as; $T_0 = 2$ and $n = 2$. It can be observed that the effect of the additional virtual disturbance is mostly absorbed and only a small amount of steady-state error remains (at the level of 2%). Finally, the effect of a mismatch in the modeled time-delay is investigated, where $T_d = 0.25$ and $L = 0.275$ corresponding to a perturbation of 10%. The results of this experiment are presented in Fig. 16. For this experiment, the values of the parameters of the local control laws and the low-pass filter $C(s)$ are, $\varepsilon = 0.0675$, $T_0 = 6$ and $n = 4$, respectively. It can be observed from Fig. 16 that the tracking error increases since the controller parameter is increased. However, the system is still stable against the mismatch in the time-delay, which illustrates the robustness of the IMPACT scheme to uncertainties in the plant model and unmodeled dynamics.

Remark 3: For the level of uncertainty considered in the results, the tracking performance of the IMPACT algorithm is comparable to approaches such as scattering [9]. However, for higher level of uncertainty especially in the time-delay, the tracking performance of the IMPACT algorithm would likely be worser. Therefore, from the results obtained in this work, the IMPACT algorithm can be considered as an alternative to such approaches.

VI. CONCLUSION

An IMPACT structure to compensate for time-delays and disturbances affecting a bilateral teleoperation system is presented in this paper. It incorporates a Smith predictor and a disturbance estimator designed for an expected class of disturbances. Both the Smith predictor and the disturbance estimator are implemented at the master side of the teleoperated system. We design local controllers for the master and slave manipulators by means of frequency response measurements and a suitable pole placement criterion. Coulomb friction is compensated by means of a suitable nonlinear feedback term in the local controllers. For formal stability analysis, the Nyquist criterion is used. There is a significant improvement in the tracking performance of the bilateral teleoperation system compared to the case when the IMPACT structure is not applied. The presented simulation results verify disturbance rejection capabilities and robustness to parametric uncertainties using our control approach. Moreover, the experimental results confirm the benefits of the algorithm against the aforementioned issues.

As the next step, the IMPACT approach should be extended to teleoperated systems featuring manipulators of nonlinear dynamics with multiple degrees-of-freedom. For this purpose, nonlinear internal model control and different type of disturbance observers can further be investigated. It could be beneficial to investigate the compensation of more complicated low velocity friction effects by means of friction observers. Furthermore, the robustness and disturbance rejection capabilities of the IMPACT approach can be investigated in other bilateral teleoperation architectures, such as force error based and 4-channel control architectures.

APPENDIX A
REFERENCE TRAJECTORY

The equations of the repetitive third order reference trajectory mentioned in Section V-C are introduced here. The acceleration of the reference trajectory is comprised of segments which are piecewise linear w.r.t. time. The equation of

the reference position is given as follows,

$$q_{ref}(t) = \begin{cases} q_{0,1}(t), & t_0 \le t \le t_1 \\ q_{1,2}(t), & t_1 < t \le t_2 \\ q_{2,3}(t), & t_2 < t \le t_3 \\ q_{3,4}(t), & t_3 < t \le t_4 \\ q_{4,5}(t), & t_4 < t \le t_5 \\ q_{5,6}(t), & t_5 < t \le t_6 \\ q_{6,7}(t), & t_6 < t \le t_7 \end{cases} \quad (53)$$

with

$$\begin{aligned} q_{0,1}(t) &= \frac{1}{6}\bar{j}\left(t^3 - t_0^3\right) + p_0, \\ q_{1,2}(t) &= \frac{1}{2}\bar{a}\left(\Delta t_1\right)^2 + v_1\Delta t_1 + p_1, \\ q_{2,3}(t) &= -\frac{1}{6}\bar{j}\left(t^3 - t_2^3\right) + \frac{1}{2}\bar{a}\left(\Delta t_2\right)^2 + v_2\Delta t_2 + p_2, \\ q_{3,4}(t) &= \bar{v}\Delta t_3 + p_3, \\ q_{4,5}(t) &= -\frac{1}{6}\bar{j}\left(t^3 - t_4^3\right) + \bar{v}\Delta t_4 + p_4, \\ q_{5,6}(t) &= -\frac{1}{2}\bar{a}\left(\Delta t_5\right)^2 + v_5\Delta t_5 + p_5, \\ q_{6,7}(t) &= \frac{1}{6}\bar{j}\left(t^3 - t_6^3\right) - \frac{1}{2}\bar{a}\left(\Delta t_6\right)^2 + v_6\Delta t_6 + p_6, \\ \Delta t_i &= t - t_i \quad \text{for} \quad i = 1, \ldots, 6 \end{aligned}$$

where $\bar{v}$, $\bar{a}$ and $\bar{j}$ represent the selected bounds on the maximum velocity, acceleration and jerk of the trajectory respectively. Furthermore, the positions $p_i = q_{ref}\left(t_i\right)$ and the velocities $v_i = \dot{q}_{ref}\left(t_i\right)$ for $i = 1, \ldots, 6$ are given as,

$$p_1 = \frac{1}{6}\bar{j}t_{\bar{j}}^3 + p_0, \quad p_2 = \frac{1}{2}\bar{a}t_{\bar{a}}^2 + v_1 t_{\bar{a}} + p_1,$$

$$p_3 = -\frac{1}{6}\bar{j}t_{\bar{j}}^3 + \frac{1}{2}\bar{a}t_{\bar{j}}^2 + v_2 t_{\bar{j}} + p_2, \quad p_4 = \bar{v}t_{\bar{v}} + p_3 \quad (54)$$

$$p_5 = -\frac{1}{6}\bar{j}t_{\bar{j}}^3 + \bar{v}t_{\bar{j}} + p_4, \quad p_6 = -\frac{1}{2}\bar{a}t_{\bar{a}}^2 + v_5 t_{\bar{a}} + p_5,$$

$$p_7 = \frac{1}{6}\bar{j}t_{\bar{j}}^3 - \frac{1}{2}\bar{a}t_{\bar{j}}^2 + v_6 t_{\bar{j}} + p_6 \quad (55)$$

$$v_1 = \frac{1}{2}\bar{j}t_{\bar{j}}^2, \quad v_2 = \bar{a}t_{\bar{a}} + v_1, \quad v_3 = \bar{v} = -\frac{1}{2}\bar{j}t_{\bar{j}}^2 + \bar{a}t_{\bar{j}} + v_2,$$

$$v_5 = -\frac{1}{2}\bar{j}t_{\bar{j}}^2, \quad v_6 = -\bar{a}t_a + v_5 \quad (56)$$

where $p_0 = q_{ref}\left(t_0\right)$ is the initial position, with

$$t_{\bar{j}} = t_1 - t_0 = t_3 - t_2 = t_5 - t_4 = t_7 - t_6 = \frac{\bar{a}}{\bar{j}}, \quad (57)$$

$$t_{\bar{a}} = t_2 - t_1 = t_6 - t_5 = \frac{v_2 - v_1}{\bar{a}}, \quad (58)$$

$$t_{\bar{v}} = t_4 - t_3 = \frac{p_4 - p_3}{\bar{v}} \quad (59)$$

which can be calculated using (54), (55) and (56). For the experimental results introduced in Section V-C, $p_0 = 0.2[\text{m}]$, $\bar{v} = 0.05[\text{m/s}]$, $\bar{a} = 0.05[\text{m/s}^2]$, and $\bar{j} = 10[\text{m/s}^3]$, respectively. Once, the algorithm is started at t_0 (i.e. t_0 is given), then the switching time instances t_i for $i = 1, \ldots, 7$ are calculated accordingly.

ACKNOWLEDGEMENT

The authors would like to thank Thomas Theunisse for helping with the experiments.

REFERENCES

[1] G. Niemeyer, C. Preusche, and G. Hirzinger, "Telerobotics," in *Springer Handbook of Robotics*, B. Siciliano and O. Khatib, Eds. Springer, 2008, pp.161–187.

[2] P. F. Hokayem and M. W. Spong, "Bilateral teleoperation: An historical survey," *Automatica*, vol. 42, no. 12, pp. 2035–2057, 2006.

[3] T. Sheridan and W. Ferrell, "Remote manipulative control with transmission delay," *IEEE Trans. Hum. Factors Electron.*, vol. 4, no. 1, pp. 25–29, 1963.

[4] P. Arcara and C. Melchiorri, "Control schemes for teleoperation with time delay: A comparative study," *Robot. Auton. Syst.*, vol. 38, no. 1, pp. 49–64, 2002.

[5] A. C. Smith and K. Hashtrudi-Zaad, "Smith Predictor Type Control Architectures for Time Delayed Teleoperation," *Int. Jour. of Rob. Res*, vol. 25, no. 8, pp. 797–818, 2006.

[6] S. K. P. Wong and D. E. Seborg, "Control strategy for single-input single-output non-linear systems with time delays," *Int. J. Control*, vol. 48, no. 6, pp. 2303–2327, 1988.

[7] C. Kravaris and R. A. Wright, "Deadtime compensation for nonlinear processes," *AIChE Journal*, vol. 35, no. 9, pp. 1535–1542, 1989.

[8] J. E. Normey-Rico and E. F. Camacho, "Dead-time compensators: A survey," *Contr. Eng. Practice*, vol. 16, no. 4, pp. 407–428, 2008.

[9] T. Miyoshi, K. Terasima, and M. Buss, "A design method of wave filter for stabilizing non-passive operating system," in *Proc. IEEE Conf. Control Appl.*, Oct. 2006, pp. 1318–1324.

[10] M. Matijević, M. Stojić, and K. Schlacher, "Absorption principle in process control applications," *Electr. Eng.*, vol. 89, no. 7, pp. 577–584, 2007.

[11] Y. Z. Tsypkin and U. Holmberg, "Robust stochastic control using the internal mode principle and internal model control," *Int. J. Control*, vol. 61, no. 4, pp. 809–822, 1995.

[12] A. Denasi, D. Kostić and, H. Nijmeijer, "An application of impact structure to bilateral teleoperations," in *Proc. IEEE Conf. Decision Control*, Dec. 2010, pp. 1985–1990.

[13] H. K. Khalil, *Nonlinear Systems*, 3rd ed. Upper Saddle River, NJ: Prentice Hall, 2002.

[14] M. M. Moghaddam and A. A. Goldenberg, "On robust control of flexible joint robots using describing function and sector bounded nonlinearity descriptions," *J. Intell. Robot. Syst.*, vol. 20, pp. 333–348, 1997.

[15] B. Bona and M. Indri, "Friction compensation in robotics: an overview," in *Proc. IEEE Conf. Decision Control*, Dec. 2005, pp. 4360–4367.

[16] G. F. Franklin, J. D. Powell, and A. Emami-Naeini, *Feedback control of dynamic systems*, 4th ed. Upper Saddle River, NJ: Prentice-Hall, 2002.

[17] M. Stojić, M. Matijević, and L. Draganović, "A robust smith predictor modified by internal models for integrating process with dead time," *IEEE Trans. Autom. Control*, vol. 46, no. 8, pp. 1293–1298, 2001.

[18] K. J. Åström and B. Wittenmark, *Computer-Controlled Systems: theory and design*, 3rd ed. Upper Saddle River, NJ: Prentice-Hall, 1997.

[19] K. Ogata, *Discrete-time control systems*, 2nd ed. Upper Saddle River, NJ, USA: Prentice-Hall, 1995.

[20] M. Morari and E. Zafiriou, *Robust Process Control*. Upper Saddle River, NJ, USA: Prentice-Hall, 1989.

[21] E. van den Ouderaa, J. Schoukens, and J. Renneboog, "Peak factor minimization, using time-frequency domain swapping algorithm," *IEEE Trans. Instrum. Meas.*, vol. 37, no. 1, pp. 144–147, 1988.

Alper Denasi received the B.Sc. and M.Sc. degrees in mechanical engineering from Istanbul Technical University, Istanbul, Turkey, in 2006, and Eindhoven University of Technology, Eindhoven, The Netherlands, in 2009, respectively. He is currently working toward the Ph.D. degree in the Dynamics and Control Group, Department of Mechanical Engineering, Eindhoven University of Technology, Eindhoven, The Netherlands. His research interests include, force/motion control of manipulators, cooperative robot manipulation, teleoperated systems.

Dragan Kostić holds PhD degree in Control technology and Robotics, received in 2004 with the Eindhoven University of Technology in The Netherlands. His expertise comprises multidisciplinary system modeling and identification, data-based control, and nonlinear control designs. Applied science is his main focus, especially in the areas of robotics and high-tech mechatronic systems. In the robotics, he investigates control and stability problems in teleoperations, cooperative control of nonholonomic mobile robots, and dynamics, balance and control of bipedal robots. In the high-tech area, he deals with multidisciplinary modeling, dynamical analysis, and high-performance control designs. His professional positions range from research and teaching at knowledge institutions till professional engineering in commercial companies.

Henk Nijmeijer (1955) obtained his MSc-degree and PhD-degree in Mathematics from the University of Groningen, Groningen, the Netherlands, in 1979 and 1983, respectively.

From 1983 untill 2000 he was affiliated with the Department of Applied Mathematics of the University of Twente, Enschede, the Netherlands. Since, 1997 he was also part-time affiliated with the Department of Mechanical Engineering of the Eindhoven University of Technology, Eindhoven, the Netherlands. Since 2000, he is a full professor at Eindhoven, and chairs the Dynamics and Control group. He has published a large number of journal and conference papers, and several books, including the 'classical' Nonlinear Dynamical Control Systems (Springer, 1990, co-author A.J.van der Schaft), with A.Rodriguez, Synchronization of Mechanical Systems (World Scientific, 2003) with R.I.Leine, Dynamics and Bifurcations of Non-Smooth Mechanical Systems (Springer-Verlag, 2004), and with A.Pavlov and N.van de Wouw, Uniform Output Regulation of Nonlinear Systems (Birkhauser 2005).

Henk Nijmeijer was editor in chief of the Journal of Applied Mathematics until 2009, corresponding editor of the SIAM Journal on Control and Optimization, and board member of the International Journal of Control, Automatica, Journal of Dynamical Control Systems, International Journal of Bifurcation and Chaos, International Journal of Robust and Nonlinear Control, Journal of Nonlinear Dynamics and the Journal of Applied Mathematics and Computer Science, and Hybrid Systems. He is a fellow of the IEEE since 2000 and was awarded in 1990 the IEE Heaviside premium. In the 2008 research evaluation of the Dutch Mechanical Engineering Departments the Dynamics and Control group was evaluated as excellent regarding all aspects (quality, productivity, relevance and viability). His research interests are in the broad scope of dynamics and control and their applications.